

Cite this: *Polym. Chem.*, 2025, **16**, 69

Influence of counterions on the thermal and solution properties of strong polyelectrolytes†

Théophile Pelras,^{*a,b} Julien Es Sayed,^{ib b} Jin Pierik,^b Andrea Giuntoli,^{ib c} Anton H. Hofman,^{ib b} Katja Loos^{ib a} and Marleen Kamperman^{ib *b}

Strong polyelectrolytes (*i.e.*, macromolecules whose charge density is independent of the medium's pH) are invaluable assets in the soft matter toolbox, as they can readily disperse in aqueous media, complex to oppositely charged species – polymers and small molecules alike – and can be implemented in a plethora of applications, ranging from surface modification to chelating agents and lubricants. However, the direct synthesis of strong polyelectrolytes in a controlled fashion remains a challenging endeavour, and their in-depth characterisation is often limited. Additionally, producing a set of charged macromolecules with the same chain length but varying counterions would open doors towards a fine control of the polymer's chemistry and physical properties. Unfortunately, this either necessitates the direct polymerisation of several monomers with potentially varying reactivities, or a time-consuming ion exchange from a single batch. Herein we explore the facile and efficient production of strong polyanions through the deprotection of a poly(3-isobutoxysulphopropyl methacrylate) using a range of inorganic and organic iodide-containing salts. Owing to the contrasting nature of their counterions, the resulting polyanions exhibit a wide range of glass transition temperatures, which follow a non-monotonic trend with increasing counterion size. While all polymers readily dissolve in water, some can also be dissolved in non-aqueous media as well. This strategy, applied to block copolymers, permits the production of a library of amphiphilic macromolecules with consistent hydrophilic and hydrophobic blocks, yet varying nature of their polyanionic segments. All amphiphiles, regardless of their counterions, readily disperse in aqueous media and form well-defined micelles featuring a hydrophobic core and a charged hydrophilic shell, as evidenced by dynamic light scattering, ζ -potential and transmission electron microscopy. Additionally, a handful of block copolymers are capable of yielding polymer micelles in organic solvents, opening an avenue to the build-up of nanostructured soft matter in non-aqueous media.

Received 29th October 2024,
Accepted 12th November 2024

DOI: 10.1039/d4py01218f

rsc.li/polymers

Introduction

Polyelectrolytes (*i.e.*, macromolecules possessing either positively or negatively charged repeating motifs throughout their chains) can readily be found in nature, where their charged character is required to fulfil specific tasks. In materials sciences, charged polymers play an important role, as they can be used in a variety of applications including energy storage and ion transport,¹ surface lubrication² and even for the stabil-

isation of micelles and other types of nanoparticles featuring a hydrophobic core.³ Additionally, when combined with an opposite-charged polymer, electrostatic interactions occur and permit the build-up of intricate nanostructures,^{4–7} the production of underwater adhesives,^{8,9} the formation of cargos for the pinpoint delivery of therapeutics^{10–12} or genetic material,^{13,14} as well as for the functionalisation of surfaces with anti-fouling properties.^{15,16}

The counterion, which is a small molecule compensating the charge of the polyionic repeating motif, is a key component of polyelectrolyte systems. Oftentimes, small-sized inorganic counterions (*e.g.*, iodide anion in quaternised amino-based polycations¹⁷ or a proton in polystyrene sulphonate¹⁸) are present, but larger organic-based ones (*e.g.*, tetra-substituted ammonium,^{19–21} oligo-ethylene glycol ammonium²¹ or imidazolium^{20,22} species) can also be featured, as their nature vastly influences the chemical and physical properties of the polymer chains.²³

Research on surfactants has already shed light on the influence of the inorganic counterions on their surface excess,^{24–26}

^aMacromolecular Chemistry and New Polymeric Materials, Zernike Institute for Advanced Materials, University of Groningen, Nijenborgh 4, 9747 AG Groningen, The Netherlands. E-mail: theophile.pelras@rug.nl, k.u.loos@rug.nl

^bPolymer Science, Zernike Institute for Advanced Materials, University of Groningen, Nijenborgh 4, 9747 AG Groningen, The Netherlands. E-mail: j.s.es.sayed@rug.nl, a.h.hofman@rug.nl, marleen.kamperman@rug.nl

^cMicromechanics, Zernike Institute for Advanced Materials, University of Groningen, Nijenborgh 4, 9747 AG Groningen, The Netherlands. E-mail: a.giuntoli@rug.nl

† Electronic supplementary information (ESI) available. See DOI: <https://doi.org/10.1039/d4py01218f>



primarily explained by their difference in size, with smaller ions possessing a larger hydration layer and therefore looser packing.²⁴ Furthermore, some organic counterions (e.g., bis(trifluoromethylsulfonyl)imide) act as plasticisers and hence reduce the glass transition temperature of polyelectrolytes. This effect is explained by the weaker ionic interactions between charged components, which cause fewer and weaker physical crosslinks within the polymer chains.^{27–29} However, while size is a key factor in determining the strength of these interactions, other intrinsic parameters of the counterion, such as symmetry, nucleophilicity, charge delocalisation and flexibility also play important roles.³⁰ Interestingly, the effect of counterion size on the glass transition temperature has been postulated to be non-monotonic, due to competing effects of electrostatic and van der Waals interactions,^{31,32} an effect that has been clearly observed in simple ionic liquids but not distinctly in poly(ionic liquids).

Beyond the fundamental research aimed at understanding the behaviour of macromolecules, the ability to readily tailor their physical properties can be exploited in applications where polymer softness is of prime importance. For instance, the introduction of plasticising counterions within polymers and ionomers lowers their glass transition temperature, which vastly increases their electronic and/or ionic conductivity.^{27–29,33–35} Furthermore, self-assembled nanoparticles can respond to the exchange of either organic or inorganic counterions. Gröschel *et al.* demonstrated the transition of nanoparticles into worm-like micelles and superstructures by a simple exchange of iodide to triiodide anions, explained by a decrease in the hydrophilicity of the polymer chains.³⁶ Another study demonstrated the transition from disk-like to worm-like micelles and later to spherical particles by introducing a variety of diamine-based counterions.³⁷

However, few studies have so far systematically investigated the effect of the nature of the counterion on the physical properties of polyelectrolytes, mostly due to the challenges of producing a large set of nearly identical macromolecules. Whilst vast developments in controlled polymerisation techniques have facilitated the production of lab-made (strong) polyelectrolytes, their synthesis with tailored chemistries and functionalities, as well as their in-depth characterisation remain challenging endeavours. Strategies to produce positively charged macromolecules often involve the quaternisation of tertiary amines^{38,39} which, albeit not always driven to completion,^{40,41} remains efficient and permits thorough analyses of the hydrophobic precursor. This route is however not as straightforward for strong polyanions *i.e.*, whose charge density is independent of the medium's pH, as they often rely on sulphonate groups that are soluble in a very limited number of media and can be incompatible with certain types of polymerisation methods. Furthermore, a systematic study of the influence of the counterion either necessitates the production of multiple polymers each requiring the same chain length, or the synthesis of one precursor whose counterion can be exchanged. The latter method is often favoured, but requires cumbersome ion exchange processes (e.g., passage through an ion exchange

membrane and extensive dialysis²¹) or the use of a large excesses of salt to induce a selective precipitation.³⁰

We have previously developed a mild yet effective strategy to produce sulphonate polymers through (i) controlled polymerisation of a protected sulphonate acrylate^{22,42} or methacrylate^{20,43} and (ii) nucleophilic deprotection using iodide-based salts. This methodology not only permits more straightforward characterisation of precursors and easier synthesis of (amphiphilic) block copolymers, but also allows the tailoring of the nature of the counterion through simple change in the nucleophile. For instance, sodium iodide typically used for the nucleophilic deprotection can be replaced by other inorganic²⁰ or inorganic^{20,22} salts while maintaining similar reaction conditions and purification protocols. To the best of our knowledge and besides our preliminary work,^{20,22} no study has yet systematically screened a wide range of counterions and investigated their effect on the thermal and solution properties of polysulphonates with constant chain lengths.

Herein, we produced an extensive range of polyelectrolytes based on poly(sulphopropyl methacrylate) (PSPMA) with the same chain length and rigidity, but featuring a variety of inorganic and organic counterions. Our previously reported methodology was employed, starting with the synthesis of a hydrophobic poly(3-isobutoxysulphopropyl methacrylate) (PBSPMA) precursor through controlled radical polymerisation, and subsequent deprotection using iodide-based nucleophiles (Scheme 1). These polyanions not only exhibit different thermal properties (*i.e.*, thermal stability and glass transition) but also solubilities. Their capacity to be dispersed in aqueous and sometimes non-aqueous media, coupled to a block copolymer synthesis strategy, was used to produce charged polymer micelles suspended in organic media.

Results and discussion

Synthesis of polyelectrolyte homopolymers

First, we employed reversible addition–fragmentation chain-transfer (RAFT) polymerisation, using a commercially available 4-cyano-4-(thiobenzoylthio)pentanoic acid chain-transfer agent (CTA) and tailor-made 3-isobutoxysulphopropyl methacrylate to produce a poly(3-isobutoxysulphopropyl methacrylate) homopolymer (PBSPMA). The isobutoxy moiety, installed on the monomer, acts as a protective group and renders the polymer hydrophobic, which greatly facilitates its synthesis as well as its characterisation prior to modification. Proton nuclear magnetic resonance (¹H NMR) spectroscopy was invoked to determine the conversion and thereby the homopolymer chain length and molecular weight ($DP_{PBSPMA} = 114$, $M_n^{PBSPMA} = 30\,400$ Da). Further ¹H NMR analyses of the purified polymer (Fig. 1A) revealed an excellent correlation between the isobutoxy protective group and alkyl spacer signals, confirming the absence of unwanted deprotection during the polymerisation. Additionally, size exclusion chromatography in *N,N*-dimethylformamide (DMF-SEC) was used to determine its dispersity ($D_{PBSPMA} = 1.10$) and verify the absence of chain–chain





Scheme 1 Tailoring the nature of the polyelectrolyte counterion through nucleophilic deprotection. (i) Controlled radical polymerisation is used to produce (ii) a protected poly(3-isobutoxysulphopropyl methacrylate) homopolymer. (iii) Subsequent nucleophilic deprotections using iodide-based salts are performed to remove the protective groups and yield (iv) a range of strong poly(sulphopropyl methacrylate) polyanions featuring various inorganic and organic counterions.

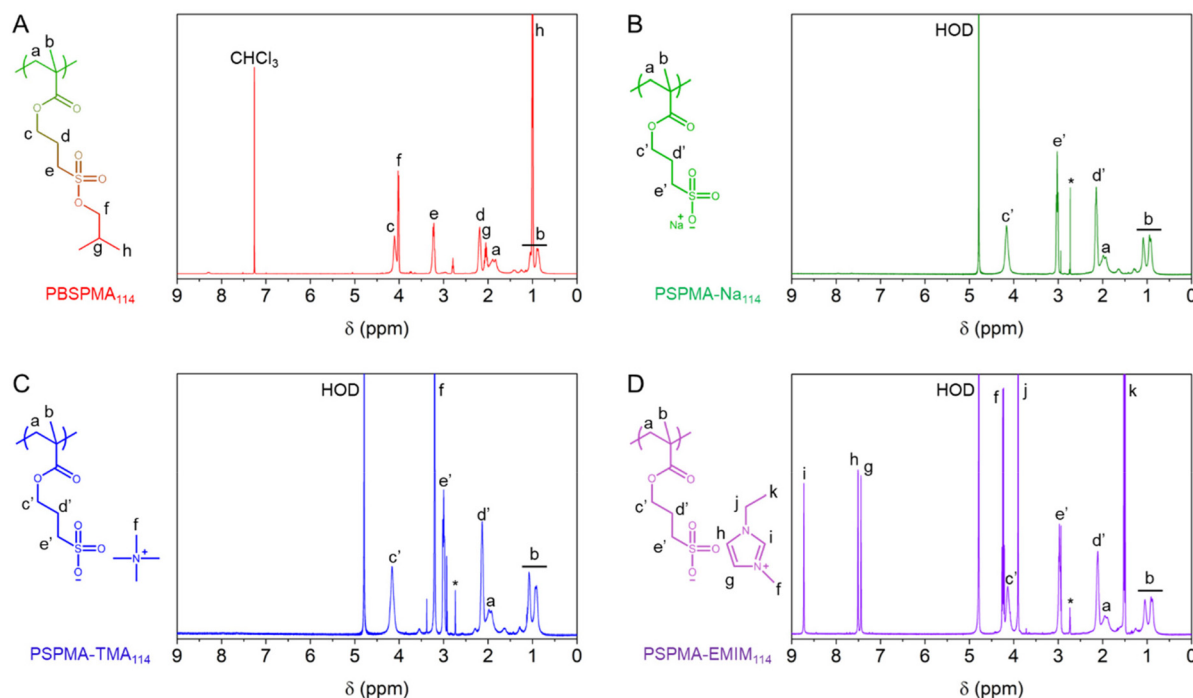


Fig. 1 Comparative ^1H NMR spectra (400 MHz) of (A) protected PBSPMA₁₁₄ and polyelectrolytes featuring various counterions, including: (B) PSPMA-Na₁₁₄, (C) PSPMA-TMA₁₁₄ and (D) PSPMA-EMIM₁₁₄.

termination (ESI Fig. S1-1†). Notably, poly(methyl methacrylate) (PMMA) was produced under similar conditions as a reference, yet yielded shorter chain length ($\text{DP}_{\text{PMMA}} = 68$, $M_n_{\text{PMMA}} = 7100$ Da), due to a lower conversion attained after 18 hours ($\text{conv.}_{\text{MMA}} = 60\%$ vs. $\text{conv.}_{\text{BSPMA}} = 96\%$, Fig. S1-2 and Table S1†).

The PBSPMA₁₁₄ homopolymer was then subjected to nucleophilic deprotection in dimethylsulphoxide (DMSO) at

70 °C for 24 hours using a variety of iodide-based salts. This enables (i) the exposure of the sulphonate groups, yielding strong polyanionic poly(sulphopropyl methacrylate) (PSPMA-R, R = counterion), and (ii) the inclusion of various inorganic and organic counterions. One advantage of this method over more time-consuming ion exchange protocols, is the straightforward purification step. Isolation of the polymer only involves a single precipitation in a non-solvent system (*i.e.*, a mixture of



n-hexane and ethanol, see the ESI for further details†), followed by a few washing cycles to remove the excess salt. The success of the deprotection reactions was confirmed by ^1H NMR, as the polymers are now soluble in D_2O , but also possess different proton signals. After reaction with sodium iodide, the spectrum of poly(sulphopropyl methacrylate) sodium salt (PSPMA- Na_{114} , Fig. 1B) *i.e.*, our benchmark polyanion, no longer features the characteristic signals from the isobutoxy protective groups (CH_2 , 2H, 4.1 ppm; CH, 1H, 2.1 ppm and CH_3 , 6H, 1.0 ppm) and only signals from the backbone and the C3 spacer ($3 \times \text{CH}_2$, 2H each, 4.2 ppm, 3.1 ppm and 2.2 ppm) are visible. Quantitative deprotection was also achieved when other iodide salts from the alkali metal group (*i.e.*, lithium iodide, potassium iodide and caesium iodide) were used *in lieu* of sodium iodide, which enables the formation of polyelectrolytes with differently sized counterions. Although the efficacy of the deprotection can still be verified by ^1H NMR (Fig. S2†), no further information about the nature of the counterion itself can be extracted using this technique.

The use of organic iodide salts however brings additional proton signals, based on the chemical nature of the counterion. A simple salt such as tetramethylammonium iodide (TMAI) only features one sharp proton signal at 3.2 ppm (originating from the four CH_3 groups of the ammonium) in the spectrum of poly(sulphopropyl methacrylate) tetramethylammonium salt (PSPMA-TMA $_{114}$, Fig. 1C). Increasing the length of the ammonium alkyl chains (*i.e.*, using tetraethylammonium iodide (TEAI) or tetrabutylammonium iodide (TBAI) to produce poly(sulphopropyl methacrylate) tetramethylammonium salt and poly(sulphopropyl methacrylate) tetrabutylammonium salt, respectively; Fig. S2†) adds additional CH_2 proton signals to the spectra. Here, ^1H NMR can be used to verify that adequate amounts of SPMA units and organic counterions are present in the samples (*i.e.*, no deficit or excess of salt is present). While a slight excess of TMA can be found in PSPMA-TMA $_{114}$, despite extensive washing cycles (1.2 : 1 salt : polymer ratio), quantitative amounts of counterions were found for the longer alkyl chains.

Furthermore, a range of iodide salts with more complex chemical structures (*i.e.*, 1-ethyl-3-methylimidazolium iodide (EMIMI), triethylphenylammonium iodide (PhTEAI), 3-(trifluoromethyl)phenyltrimethylammonium iodide (FPhTMAI) and butylthiocholine iodide (BTCl)) were used for nucleophilic deprotection. Again, the success of the deprotection can be assessed not only by the loss of the isobutoxy protective groups, but also by the presence of the organic counterions. For instance, poly(sulphopropyl methacrylate) 1-ethyl-3-methylimidazolium salt (PSPMA-EMIM $_{114}$, Fig. 1D) features very distinct signals from the imidazolium ring ($3 \times \text{CH}$, 1H each, 8.8 ppm, 7.5 ppm and 7.4 ppm), while poly(sulphopropyl methacrylate) 3-(trifluoromethyl)phenyltrimethylammonium salt (PSPMA-FPhTMA $_{114}$, Fig. S2†) features aromatic (4H, 7.8–8.3 ppm) and methyl ammonium (CH_3 , 12H, 3.7 ppm) signals. Interestingly, fluorine nuclear magnetic resonance (^{19}F NMR) spectroscopy was also conducted on PSPMA-FPhTMA $_{114}$ and the pristine salt (Fig. S3†). Both species exhibited fluorine signals at ~ -62 ppm, further con-

firmed the presence of the fluorinated counterion in the polyelectrolyte.

Albeit neither quantitative nor as precise as ^1H NMR, Fourier transform infrared (FTIR) spectroscopy was also used to characterise the various polyelectrolytes (Fig. S4†). All the polymers feature typical $\text{S}=\text{O}$ stretching at 1045 and 1192 cm^{-1} after deprotection, and some include signals that are specific to their counterions, such as the $\text{C}-\text{F}$ stretching mode of PSPMA-FPhTMA $_{114}$ at 1324 cm^{-1} or the $\text{C}=\text{O}$ ketone of poly(sulphopropyl methacrylate) butylthiocholine salt (PSPMA-BTC $_{114}$) stretching at 1699 cm^{-1} .

Due to their charged nature and to the absence of large hydrophobic spacers, our polyelectrolytes can no longer be dissolved in DMF, so aqueous SEC (Fig. S5†) was used to verify that nucleophilic deprotections did not affect the integrity of the polymer chains. Except for of PSPMA-FPhTMA $_{114}$ (possibly due to interaction with the column material³⁰), all samples feature a monomodal peak, which confirms the absence of side-reactions during deprotection. The various polyelectrolytes also possess the same retention volume and similar molecular weights, as observed elsewhere,²¹ which suggests little influence of the nature and size of the counterion on the polymer coil size and polymer-solvent interaction.

Thermal and solution properties of polyelectrolyte homopolymers

As evidenced in previous studies,^{22,44} the nature of the counterion, particularly inorganic *vs.* organic, strongly affects the thermal properties of a polyelectrolyte. Therefore, the thermal stability and the presence of transition temperatures were investigated by thermogravimetric analysis (TGA) and differential scanning calorimetry (DSC), respectively, and compared to those of the PBSPMA $_{114}$ and PMMA $_{68}$ reference materials. The protected homopolymer is typically stable up to a temperature of ~ 180 $^{\circ}\text{C}$, after which it decomposes with an initial loss of mass of ~ 15 – 20% , attributed to the removal of the isobutoxy protective groups. Further loss of mass occurs at ~ 200 $^{\circ}\text{C}$ through acid-catalysed hydrolysis of the acrylic ester,⁴⁶ before the final degradation of the backbone around ~ 400 $^{\circ}\text{C}$ (Fig. S6-1†).

While all samples featuring inorganic counterions are now stable up to 200–250 $^{\circ}\text{C}$ (excluding the evaporation of trace amounts of solvent, Fig. 2A and ESI S7†), their decomposition still occurs through a multi-step process.⁴⁴ Interestingly, PSPMA-K $_{114}$ features an early loss of mass at 210 $^{\circ}\text{C}$, while other polyanions only start to degrade at 250–270 $^{\circ}\text{C}$; therefore, their thermal stability is not entirely dictated by the size of the counterion. While the protected precursor almost fully degrades before reaching the maximal temperature of 700 $^{\circ}\text{C}$, polyelectrolytes with inorganic counterions retain a large weight fraction, and the heavier the cation is (*i.e.*, lower in the alkali metal group), the greater the weight percentage remaining at the end of the ramp. The residues at the end of the heating ramp typically consist of complex salts/ceramics that are not volatile in the measured temperature range. Most





Fig. 2 Thermogravimetric and differential scanning calorimetry analyses of the polyelectrolyte homopolymers. (A) TGA and (B) DSC of polyelectrolytes with inorganic counterions: PSPMA-Li₁₁₄ (red), PSPMA-Na₁₁₄ (orange), PSPMA-K₁₁₄ (green) and PSPMA-Cs₁₁₄ (blue). (C) TGA and (D) DSC of polyelectrolytes with simple quaternary ammonium counterions: PSPMA-TMA₁₁₄ (red), PSPMA-TEA₁₁₄ (orange) and PSPMA-TBA₁₁₄ (green). (E) TGA and (F) DSC of polyelectrolytes with other organic counterions: PSPMA-EMIM₁₁₄ (red), PSPMA-PhTMA₁₁₄ (orange), PSPMA-FPhTEA₁₁₄ (green) and PSPMA-BTC₁₁₄ (blue).

notably however, no thermal events occurred for any of the inorganic counterions (Fig. 2B), while the PBSPMA₁₁₄ precursor exhibited a glass transition temperature ($T_{g, \text{PBSPMA}} = 16.7^\circ\text{C}$, Fig. S6-2†). This absence of a T_g in the measured range, previously observed for both acrylic^{22,42} and methacrylic^{20,43} systems, is consistent with the brittle nature of polyelectrolytes, which can possess glass transition temperatures up to 228°C ,³¹ exceeding the capability of our instrument and the thermal stability of our polymers.

The presence of an organic counterion appears to greatly decrease the thermal stability of the polyelectrolyte to $150\text{--}170^\circ\text{C}$, without any remarkable trend (Fig. 2C and E). However, the fully organic nature of the polyelectrolytes permits their complete decomposition with a remaining char weight $\leq 5\text{ wt\%}$, thus the salts that are formed upon heating are somewhat more volatile and do not yield complex salts/ceramics.⁴⁴ Most importantly however, new glass transition temperatures, generally below room temperature, appear for most



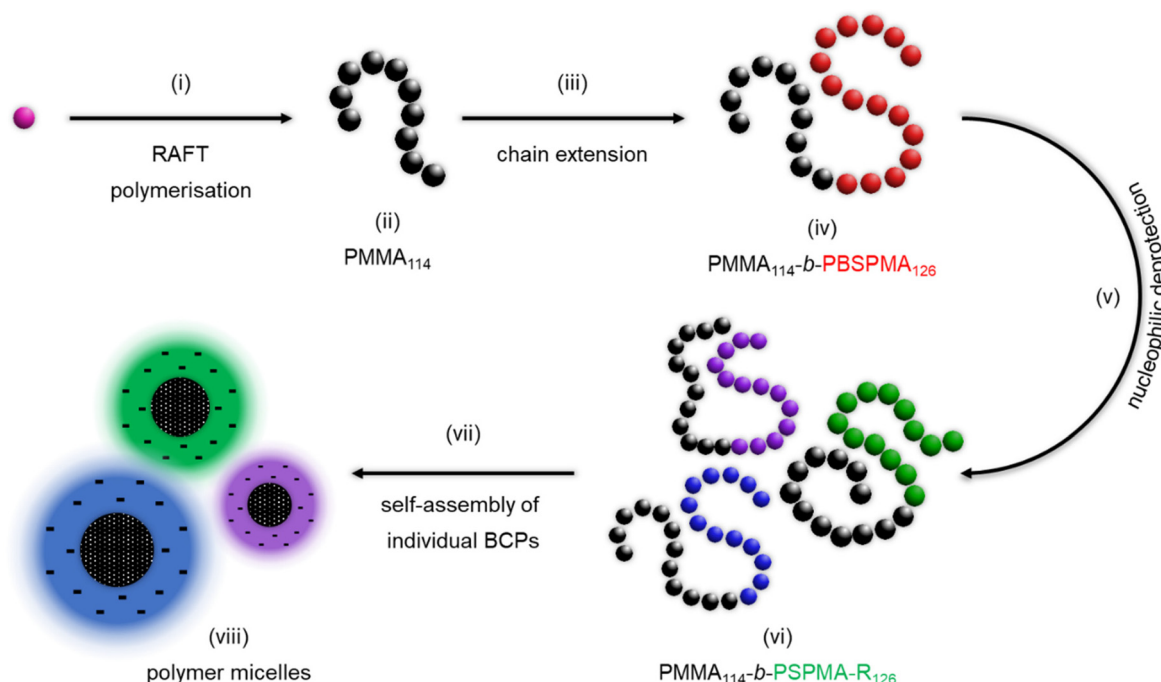
polyelectrolytes with organic counterions, akin to the plasticising effect observed in poly(ionic liquids).⁴⁵ The only outlier, PSPMA-TMA₁₁₄, remains brittle and does not exhibit any T_g in the measured temperature range, while longer alkyl analogues do possess one, also affected by the number of carbons ($T_{g, \text{PSPMA-TEA}} = -12.6$ °C and $T_{g, \text{PSPMA-TBA}} = 2.7$ °C, Fig. 2D). Other organic counterions also provide the polyelectrolyte with a T_g ranging from -50.2 °C for PSPMA-EMIM₁₁₄ to 55.1 °C for poly(sulphopropyl methacrylate) phenyltriethyl ammonium salt (PSPMA-PhTEA₁₁₄, Fig. 2F and Table S4†).

The exact relationship between the counterion and the observed glass transition temperature is however difficult to pinpoint, as several competing effects may be at stake. The size of the hydration layer around the counterion,²⁴ a plasticising effect due to weaker ion/counterion interactions,^{27–29} or intrinsic parameters such as symmetry, nucleophilicity and the charge delocalisation³⁰ may all play important and possibly contradictory roles. As a general observation, the glass transition temperature seems to be very high for small inorganic counterions, decreasing sharply for sufficiently large

Table 1 Solubility tests of PSPMA-R homo-polyelectrolytes featuring various counterions

Polyelectrolyte	Water	DMSO	Methanol	Ethanol	Acetone	THF	ACN
PSPMA-Li ₁₁₄	o	p*	p*	p*	x	x	x
PSPMA-Na ₁₁₄	o	p*	x	X	x	x	x
PSPMA-K ₁₁₄	o	x	x	x	x	x	x
PSPMA-Cs ₁₁₄	o	p*	x	x	x	x	x
PSPMA-TMA ₁₁₄	o	p*	p*	x	x	x	x
PSPMA-TEA ₁₁₄	o	p*	p*	o	x	x	p
PSPMA-TBA ₁₁₄	o	p*	p*	o	o	x	p
PSPMA-EMIM ₁₁₄	o	o	o	o	x	x	p
PSPMA-PhTEA ₁₁₄	o	o	o	o	x	x	p
PSPMA-FPhTMA ₁₁₄	o	o	o	p*	x	x	x
PSPMA-BTC ₁₁₄	o	o	o	p*	x	x	p

Qualitative assessment of the solubility at 25 °C with concentration kept at 5 g L⁻¹ across the whole series. o: fully soluble. p: partially soluble (*i.e.*, particles and hair-like aggregates can be seen by eye). p*: partially soluble in neat solvent and soluble in 'wet' solvent (*i.e.*, 10–20 vol% water). x: insoluble.



Scheme 2 Synthesis of hydrophobic/strong anionic amphiphilic block copolymers capable of self-assembly in aqueous or organic media. (i) Controlled radical polymerisation is used to produce (ii) a poly(methyl methacrylate) segment, which is (iii) chain extended to yield (iv) a protected poly(methyl methacrylate)-*block*-poly(3-isobutoxysulphopropyl methacrylate) hydrophobic block copolymer. (v) Nucleophilic deprotection is then performed to produce (vi) a range of poly(methyl methacrylate)-*block*-poly(sulphopropyl methacrylate) amphiphiles, (vii) capable of self-assembly in various media to produce (viii) polymer micelles with consistent hydrophobic cores and varying natures of their charged shells.



organic counterions but increasing again for even larger species. These findings are in line with the empirical model proposed by Bocharova *et al.*,³¹ which predicts a non-monotonic dependence of T_g on the molecular volume V_m (*i.e.*, the volume of the monomer unit + counterion complex) based on the competing contributions of electrostatic ($\sim V_m^{-1/3}$) and van der Waals ($\sim V_m^{2/3}$) interactions. Interestingly, this non-monotonic behaviour is predicted by molecular dynamics simulations^{32,33} and has been clearly observed in simple ionic liquids, while the presence of a clear minimum is not obvious for polymeric ionic liquids. Admittedly, only TMA^+ , TEA^+ , and TBA^+ are the three counterions with a clearly defined trend in molecular volume V_m , and the difference in T_g between TEA^+ and TBA^+ ($\sim 15^\circ\text{C}$) is significant but not larger than the fluctuations in data reported in previous literature.³¹ A larger difference in the T_g ($\sim 100^\circ\text{C}$) is observed for the large organic counterions EMIM, PhTMA and FPhTEA, but their complex structure makes it challenging to estimate and compare their molecular volumes.

A change in the counterion, while having large repercussions on the thermal behaviour of the polyelectrolytes, also greatly influences their ability to be dissolved in non-aqueous solvents. While apolar solvents such as *n*-hexane or cyclohexane cannot dissolve any of the polyelectrolytes featured in this study, a series of polar solvents were selected and solubility tests were conducted (Table 1 and Fig. S8-1†). Inorganic counterions do not provide solubility in organic solvents, except for 'wet' DMSO (*i.e.*, DMSO with 10–20 vol% water, also used as a medium for the deprotection reaction) and only PSPMA- Li_{114} can be dissolved in 'wet' methanol and ethanol. Surprisingly, PSPMA- K_{114} did not dissolve at all in DMSO, as evidenced during deprotection, when the polymer precipitated over the course of the reaction. Note that this phenomenon does not hinder full deprotection, as shown previously using acetone *i.e.*, another non-solvent for PSPMA-Na as medium.⁴³

Polyelectrolytes with simple counterions (*i.e.*, PSPMA- TMA_{114} , PSPMA- TEA_{114} and PSPMA- TBA_{114}) also dissolve in 'wet' DMSO, in 'wet' methanol and in dry ethanol for longer alkane chains, while larger cations (*i.e.*, EMIM⁺, PhTEA⁺, FPhTMA⁺ and BTC⁺) permit dissolution in neat solvents. Aprotic polar organics (*i.e.*, acetone, tetrahydrofuran and acetonitrile) provide little ability to dissolve the polyelectrolytes, except for PSPMA- TBA_{114} , which disperses into acetone (see ESI†). To further confirm the capacity of some organic solvents to dissolve polyelectrolytes, ^1H NMR spectra were recorded in DMSO- d_6 , methanol- d_4 , ethanol- d_6 and acetone- d_6 (Fig. S2†). For all polyelectrolytes, the relative integration of signals was maintained, and no peak broadening was observed, confirming their solubility in these organic solvents.

Synthesis and self-assembly of block copolymers

To expand our study, a series of amphiphilic block copolymers (BCPs) featuring a hydrophobic block and a hydrophilic PSPMA-R segment were produced *via* sequential RAFT polymerisation, followed by nucleophilic deprotection (Scheme 2). A poly(methyl methacrylate) macro-CTA was synthesised (PMMA₁₁₄, M_n SEC = 11 400 Da, \bar{D} = 1.27) and chain extended

with our protected sulphonate monomer, yielding an organo-soluble protected precursor (PMMA₁₁₄-*b*-PBSPMA₁₂₆, M_n SEC+NMR = 44 800, \bar{D} = 1.18) that is straightforward to characterise (Fig. S9-1†). ^1H NMR analysis of the purified BCP confirmed the successful addition of BSPMA units onto the PMMA₁₁₄ segment and enabled an accurate calculation of the chain length of the second block by comparing the PBSPMA CH₂ signals (2H, 4.2 ppm, 2H, 3.2 ppm and 2H, 2.2 ppm) to the PMMA methyl signal (3H, 3.6 ppm). Note that a consistent



Fig. 3 Influence of the type of counterion on the glass transition temperature of the block copolymers. (A) DSC thermograms of PMMA₁₁₄ (black), PMMA₁₁₄-*b*-PBSPMA₁₂₆ (red) and PMMA₁₁₄-*b*-PSPMA-Na₁₂₆ (green). (B) DSC thermograms of PMMA₁₁₄-*b*-PSPMA-TMA₁₂₆ (red), PMMA₁₁₄-*b*-PSPMA-TEA₁₂₆ (orange) and PMMA₁₁₄-*b*-PSPMA-TBA₁₂₆ (green). (C) DSC thermograms of PMMA₁₁₄-*b*-PSPMA-EMIM₁₂₆ (red), PMMA₁₁₄-*b*-PSPMA-PhTEA₁₂₆ (orange), PMMA₁₁₄-*b*-PSPMA-FPhTMA₁₂₆ (green) and PMMA₁₁₄-*b*-PSPMA-BTC₁₂₆ (blue).



ratio was found between the PBSPMA isobutoxy CH_3 signal (6H, 1.0 ppm) and abovementioned CH_2 signals, which confirms that the isobutoxy protective groups are preserved during chain extension. Furthermore, SEC corroborated the quantitative chain extension, with a full shift of the polymer signal towards a lower retention volume/higher molecular weight, as well as the absence of chain–chain termination.

Then, a series of nucleophilic deprotections were conducted with most of the iodide-based salts, which enabled the

production of BCPs with a constant PMMA molar fraction ($x_{\text{PMMA}} = 0.48$) but varied the nature of the polyelectrolyte. The successful deprotections, albeit established on homopolymers, were verified using ^1H NMR (Fig. S9†) by monitoring the disappearance of the isobutoxy protective groups and, if applicable, the presence of new proton signals from the organic counterions. Once the chemical nature of the deprotected block copolymers was verified, the effect of the various counterions on the overall thermal behaviour was investigated

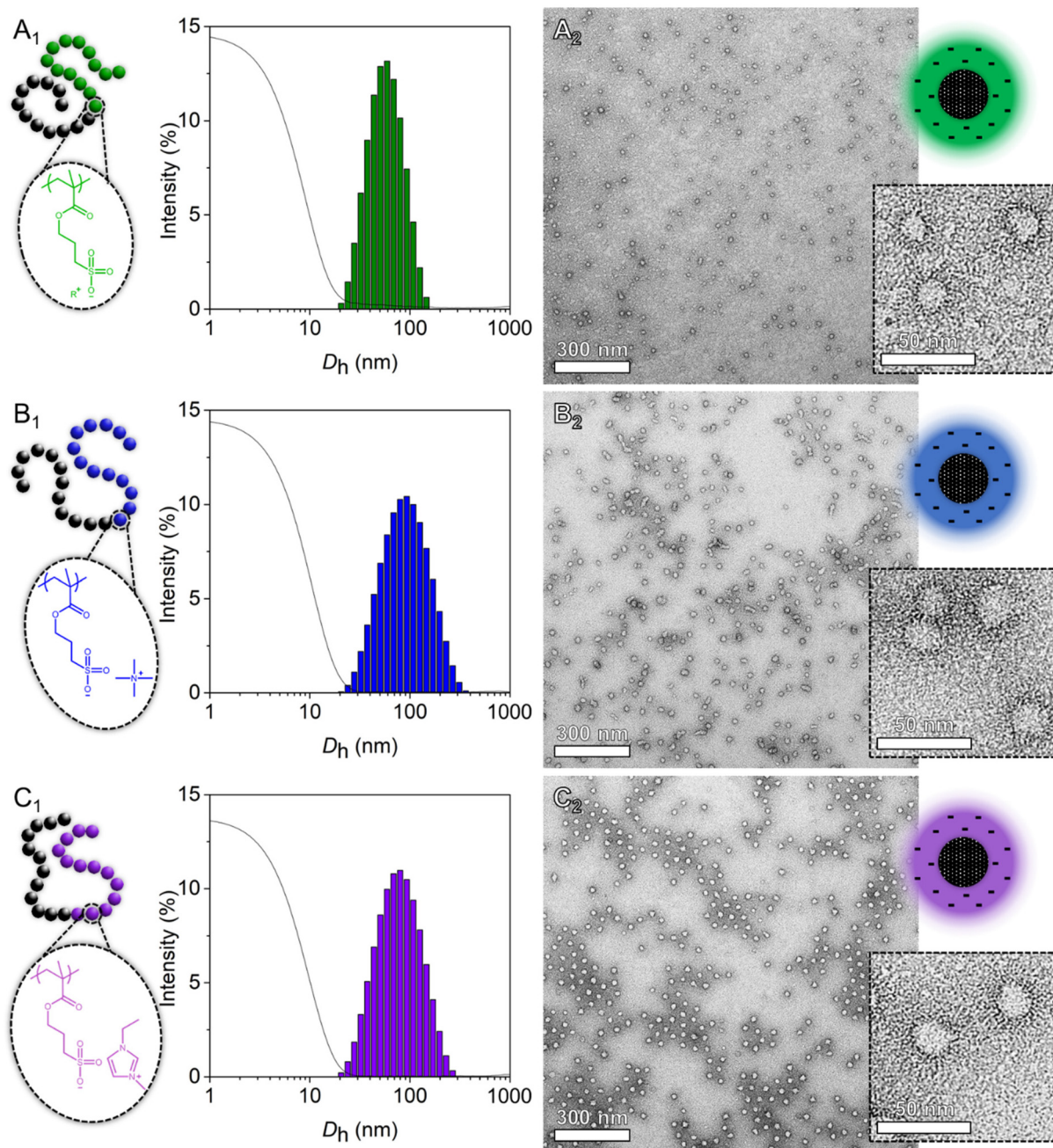


Fig. 4 Self-assembly of selected amphiphilic block copolymers in aqueous media. (A_1 – C_1) DLS size distribution plots (bars) and corresponding correlograms (solid lines) and (A_2 – C_2) negatively stained TEM images of polymer micelles obtained from $\text{PMMA}_{114}\text{-}b\text{-PSPMA-Na}_{126}$ (green), $\text{PMMA}_{114}\text{-}b\text{-PSPMA-TMA}_{126}$ (blue) and $\text{PMMA}_{114}\text{-}b\text{-PSPMA-EMIM}_{126}$ (purple) at 1 g L^{-1} in 10 mM KNO_3 .





Fig. 5 Comparative self-assembly of amphiphilic block copolymers in various types of media. Negatively stained TEM images of polymer micelles obtained from (A) PMMA₁₁₄-*b*-PSPMA-EMIM₁₂₆, (B) PMMA₁₁₄-*b*-PSPMA-PhTEA₁₂₆, (C) PMMA₁₁₄-*b*-PSPMA-FPhTMA₁₂₆ and (D) PMMA₁₁₄-*b*-PSPMA-BTC₁₂₆ in 10 mM KNO₃, methanol or ethanol.



using DSC. While PBSPMA and PMMA possess vastly different glass temperatures ($T_{\text{g PBSPMA}} = 16.7\text{ }^{\circ}\text{C}$ vs. $T_{\text{g PMMA}} = 108\text{ }^{\circ}\text{C}$), a single T_{g} was observed for the protected block copolymer ($T_{\text{g BCP}} = 18.1\text{ }^{\circ}\text{C}$, Fig. 3A). This could indicate a mixed phase, albeit not in agreement with the volume fractions of the blocks and the Flory–Fox equation. Previous studies on acrylic analogues^{22,42} also evidenced this behaviour, where two separate T_{g} were observed for block copolymers with a low protected sulphonate content, and a single one close to that of the sulphonate homopolymer when this ratio increased. Therefore, we suggest that both blocks are capable of phase separation, but with a short-range order only. Upon nucleophilic deprotection with NaI or TMAI, no T_{g} can be detected in the thermograms of the BCPs, despite the PMMA block remaining pristine during the deprotection, a behaviour that has also been evidenced before.^{22,42} However, the presence of larger counterions, introduces new glass transition temperatures, ranging from 18.6 to 73.1 $^{\circ}\text{C}$ (Fig. 3 and Table S5†). The values appear to be in part dictated by the nature of the counterion and to lie between those of a polyelectrolyte homopolymer and the PMMA block, in line with the Flory–Fox equation. For instance, the glass transition temperatures of the PMMA₁₁₄ and PSPMA-PhTEA₁₂₆ homopolymers are $T_{\text{g PMMA}} = 108\text{ }^{\circ}\text{C}$ and $T_{\text{g PSPMA-PhTEA}} = 11.7\text{ }^{\circ}\text{C}$, respectively, while that of the PhTEA-based block copolymer is measured at 68.6 $^{\circ}\text{C}$. This could be indicative of a single mixed phase between PMMA and any of the polyelectrolytes featuring organic counterions.⁴⁷ Comparative DSC thermograms of the PMMA₁₁₄ macro-CTA, polyelectrolytes and deprotected BCPs are available in Fig. S10†.

The amphiphilic nature of these BCPs allows them to self-assemble in aqueous media. To enable the screening of the polyelectrolyte segments and hence reduce particle aggregation (*i.e.*, slow diffusion mode),⁴⁸ a small amount of salt was added. The ‘direct dissolution’ method was employed (*i.e.*, an appropriate volume of 10 mM KNO₃ was charged into a vial loaded with dried BCP to achieve a 1 g L^{−1} concentration), which readily enabled the formation of micelles with a hydrophobic core and a negatively charged hydrophilic shell, as evidenced by ζ -potential measurements (Table S6†). Dynamic light scattering (DLS, Fig. 4 and Fig. S11†) revealed the presence of polymer micelles with hydrodynamic diameters between $D_{\text{h}} = 50\text{--}75\text{ nm}$ and relatively narrow polydispersity indices $\text{PDI} \approx 0.2$ for all but one block copolymer. Only the FPhTMA-based BCP possesses a larger mean particle diameter and polydispersity index ($D_{\text{h BCP-FPhTMA}} = 95\text{ nm}$, $\text{PDI}_{\text{BCP-FPhTMA}} = 0.383$), suggesting a slight inhomogeneity in the self-assembly process. Transmission electron microscopy (TEM, Fig. 4 and Fig. S12†) was used to visualise the particles, aided by the application of a negative stain. Here the PMMA core (*i.e.*, low electron density) appears bright, while the uranyl acetate stain (*i.e.*, high electron density) penetrates the negatively charged shell of the micelles, thus appearing dark. All amphiphilic BCPs form well-defined spherical micelles in aqueous media, once more suggesting that the counterions have little influence on the self-assembly mechanism. A few elongated or fused

micelles within a sphere-dominated population were observed for the PMMA₁₁₄-*b*-PSPMA-FPhTMA₁₂₆ block copolymer, in accordance with the larger D_{h} and PDI values measured by dynamic light scattering.

With some of the polyelectrolytes possessing the ability to dissolve in non-aqueous solvents, attempts have been made to produce nanoparticles in organic media using the same ‘direct dissolution’ method. The key to this protocol lies in the choice of the medium, one that would enable the dissolution of the polyelectrolyte domain but not of the PMMA segment. As such, acetone, acetonitrile, DMSO and THF are incompatible, while methanol and ethanol remain potential candidates. Multiple populations, large dispersity indices and poor correlograms were measured by DLS for all samples dispersed in methanol (Fig. S13†) and for most dispersed in ethanol (Fig. S14†), suggesting non-homogeneous self-assembly in those media. Nonetheless, negatively stained specimens were prepared and imaged using TEM (Fig. S15 and Fig. S16†). Through a direct comparison with polymer micelles self-assembled in aqueous media (Fig. 5), it is evident that methanol and ethanol, albeit usable solvents for the formation of aggregates, do not permit the fabrication of particles with homogeneous shapes and narrow polydispersities. Often, very large and ill-formed particles are present within populations of small spherical micelles, and a few worm-like specimens were observed (*i.e.*, PMMA₁₁₄-*b*-PSPMA-EMIM₁₂₆ in methanol and PMMA₁₁₄-*b*-PSPMA-EMIM₁₂₆ in ethanol). This might be explained by the limited solubility of PMMA in these solvents and/or by their low dielectric constant, resulting in limited charge repulsion between the charged coronas of the particles and therefore poor dispersion.^{49,50}

Conclusion & outlook

Herein, we report a simple yet effective methodology to produce polyelectrolytes featuring a range of counterions, from simple alkali metals to more complex organic salts. The nature of the counterion has a strong effect on the thermal stability, on the presence of a glass transition temperature, as well as on the solubility of the polyelectrolytes. Polyelectrolytes including inorganic counterions tend to have a higher thermal stability, but exhibit no phase transition and lack solubility in organic solvents. Larger organic counterions on the other hand provide a wide range of glass transition temperatures, which appear to follow a non-monotonic trend with respect to counterion size, and provide moderate solubility in polar organics.

Our strategy also permits the production of copolymers, including a hydrophobic block and a polyelectrolyte segment. The protected diblock precursors are fully hydrophobic, which facilitates their characterisation, yet tailoring the counterion relies on the simple choice of a nucleophile during deprotection. All the amphiphilic block copolymers readily self-assemble into spherical micelles in aqueous media, with similar hydrodynamic diameters and relatively narrow polydis-



persities. The dispersion of some copolymers in methanol and ethanol has been attempted, and while our system does not exhibit consistent formation of well-defined polymer micelles, it opens up avenues for the design of structured soft matter outside the boundaries of aqueous media.

Author contributions

The manuscript was written through contributions of all the authors. All the authors have approved the final version of the manuscript.

Data availability

The data supporting this article (Materials and methods, as well as additional ^1H NMR spectra, SEC elugrams, DSC, and TGA thermograms, DLS plots, and TEM images) have been included as part of the ESI.†

Conflicts of interest

There are no conflicts to declare.

Acknowledgements

The authors warmly thank Jur van Dijken, Léon Rohrbach and Dr Marc C. A. Stuart for their technical assistance with thermogravimetric analyses, aqueous size exclusion chromatography, and electron microscopy, respectively. This research received funding from the Dutch Research Council (NWO) in the framework of the ENW PPP Fund for the top sectors and from the Ministry of Economic Affairs in the framework of the 'PPS-Toeslagregeling'. M. K. is the grateful recipient of a European Research Council grant (European Union's Horizon 2020 research and innovation program, consolidator grant agreement no. 864982). T.P. warmly thanks Uluru.

References

- 1 M. Armand and J. M. Tarascon, Building better batteries, *Nature*, 2008, **451**(7179), 652–657.
- 2 U. Raviv, S. Giasson, N. Kampf, J.-F. Gohy, R. Jérôme and J. Klein, Lubrication by charged polymers, *Nature*, 2003, **425**(6954), 163–165.
- 3 J. Kötz, S. Kosmella and T. Beitz, Self-assembled polyelectrolyte systems, *Prog. Polym. Sci.*, 2001, **26**(8), 1199–1232.
- 4 T. Pelras, Nonappa, C. S. Mahon and M. Müllner, Cylindrical Zwitterionic Particles via Interpolyelectrolyte Complexation on Molecular Polymer Brushes, *Macromol. Rapid Commun.*, 2021, **42**(8), 2000401.
- 5 T. Pelras, C. S. Mahon, Nonappa, O. Ikkala, A. H. Gröschel and M. Müllner, Polymer Nanowires with Highly Precise Internal Morphology and Topography, *J. Am. Chem. Soc.*, 2018, **140**(40), 12736–12740.
- 6 T. I. Löbbling, J. S. Haataja, C. V. Synatschke, F. H. Schacher, M. Müller, A. Hanisch, A. H. Gröschel and A. H. E. Müller, Hidden Structural Features of Multicompartment Micelles Revealed by Cryogenic Transmission Electron Tomography, *ACS Nano*, 2014, **8**(11), 11330–11340.
- 7 J.-M. Malho, M. Morits, T. I. Löbbling, Nonappa, J. Majoinen, F. H. Schacher, O. Ikkala and A. H. Gröschel, Rod-Like Nanoparticles with Striped and Helical Topography, *ACS Macro Lett.*, 2016, **5**(10), 1185–1190.
- 8 L. van Westerveld, J. Es Sayed, M. de Graaf, A. H. Hofman, M. Kamperman and D. Parisi, Hydrophobically modified complex coacervates for designing aqueous pressure-sensitive adhesives, *Soft Matter*, 2023, **19**(45), 8832–8848.
- 9 L. van Westerveld, T. Pelras, A. H. Hofman, K. Loos, M. Kamperman and J. Es Sayed, Effect of Polyelectrolyte Charge Density on the Linear Viscoelastic Behavior and Processing of Complex Coacervate Adhesives, *Macromolecules*, 2024, **57**(2), 652–663.
- 10 M. Li, W. Song, Z. Tang, S. Lv, L. Lin, H. Sun, Q. Li, Y. Yang, H. Hong and X. Chen, Nanoscaled Poly(l-glutamic acid)/Doxorubicin-Amphiphile Complex as pH-responsive Drug Delivery System for Effective Treatment of Nonsmall Cell Lung Cancer, *ACS Appl. Mater. Interfaces*, 2013, **5**(5), 1781–1792.
- 11 W. S. Cheow and K. Hadinoto, Self-assembled amorphous drug-polyelectrolyte nanoparticle complex with enhanced dissolution rate and saturation solubility, *J. Colloid Interface Sci.*, 2012, **367**(1), 518–526.
- 12 S. Kamble, P. Varamini, M. Müllner, T. Pelras and R. Rohanizadeh, Bisphosphonate-functionalized micelles for targeted delivery of curcumin to metastatic bone cancer, *Pharm. Dev. Technol.*, 2020, **25**(9), 1118–1126.
- 13 Y. Chen, D. Diaz-Dussan, Y.-Y. Peng and R. Narain, Hydroxyl-Rich PGMA-Based Cationic Glycopolymers for Intracellular siRNA Delivery: Biocompatibility and Effect of Sugar Decoration Degree, *Biomacromolecules*, 2019, **20**(5), 2068–2074.
- 14 B. S. Kim, S. Chuanoi, T. Suma, Y. Anraku, K. Hayashi, M. Naito, H. J. Kim, I. C. Kwon, K. Miyata, A. Kishimura and K. Kataoka, Self-Assembly of siRNA/PEG-b-Cationomer at Integer Molar Ratio into 100 nm-Sized Vesicular Polyion Complexes (siRNAsomes) for RNAi and Codelivery of Cargo Macromolecules, *J. Am. Chem. Soc.*, 2019, **141**(8), 3699–3709.
- 15 A. M. C. Maan, A. H. Hofman, T. Pelras, I. M. Ruhof, M. Kamperman and W. M. de Vos, Toward Effective and Adsorption-Based Antifouling Zipper Brushes: Effect of pH, Salt, and Polymer Design, *ACS Appl. Polym. Mater.*, 2023, **5**(10), 7968–7981.
- 16 A. M. C. Maan, C. N. Graafsma, A. H. Hofman, T. Pelras, W. M. de Vos and M. Kamperman, Scalable Fabrication of Reversible Antifouling Block Copolymer Coatings via Adsorption Strategies, *ACS Appl. Mater. Interfaces*, 2023, **15**(15), 19682–19694.



- 17 C. V. Synatschke, T. I. Löbbling, M. Förtsch, A. Hanisch, F. H. Schacher and A. H. E. Müller, Micellar Interpolyelectrolyte Complexes with a Compartmentalized Shell, *Macromolecules*, 2013, **46**(16), 6466–6474.
- 18 J. E. Coughlin, A. Reisch, M. Z. Markarian and J. B. Schlenoff, Sulfonation of polystyrene: Toward the “ideal” polyelectrolyte, *J. Polym. Sci., Part A: Polym. Chem.*, 2013, **51**(11), 2416–2424.
- 19 P. M. Reichstein, J. C. Brendel, M. Drechsler and M. Thelakkat, Poly(3-hexylthiophene)-block-poly(tetrabutylammonium-4-styrenesulfonate) Block Copolymer Micelles for the Synthesis of Polymer Semiconductor Nanocomposites, *ACS Appl. Nano Mater.*, 2019, **2**(4), 2133–2143.
- 20 A. H. Hofman, M. Pedone and M. Kamperman, Protected Poly(3-sulfopropyl methacrylate) Copolymers: Synthesis, Stability, and Orthogonal Deprotection, *ACS Polym. Au*, 2022, **2**(3), 169–180.
- 21 G. J. Tudryn, W. Liu, S.-W. Wang and R. H. Colby, Counterion Dynamics in Polyester–Sulfonate Ionomers with Ionic Liquid Counterions, *Macromolecules*, 2011, **44**(9), 3572–3582.
- 22 T. Pelras, A. H. Hofman, L. M. H. Germain, A. M. C. Maan, K. Loos and M. Kamperman, Strong Anionic/Charge-Neutral Block Copolymers from Cu(0)-Mediated Reversible Deactivation Radical Polymerization, *Macromolecules*, 2022, **55**(19), 8795–8807.
- 23 A. Kisliuk, V. Bocharova, I. Popov, C. Gainaru and A. P. Sokolov, Fundamental parameters governing ion conductivity in polymer electrolytes, *Electrochim. Acta*, 2019, **299**, 191–196.
- 24 K. Lunkenheimer, D. Prescher and K. Geggel, Role of Counterions in the Adsorption and Micellization Behavior of 1 : 1 Ionic Surfactants at Fluid Interfaces—Demonstrated by the Standard Amphiphile System of Alkali Perfluoro-n-octanoates, *Langmuir*, 2022, **38**(3), 891–902.
- 25 K. Lunkenheimer, K. Geggel and D. Prescher, Role of Counterion in the Adsorption Behavior of 1 : 1 Ionic Surfactants at Fluid Interfaces—Adsorption Properties of Alkali Perfluoro-n-octanoates at the Air/Water Interface, *Langmuir*, 2017, **33**(39), 10216–10224.
- 26 K. Lunkenheimer, D. Prescher, R. Hirte and K. Geggel, Adsorption Properties of Surface Chemically Pure Sodium Perfluoro-n-alkanoates at the Air/Water Interface: Counterion Effects within Homologous Series of 1 : 1 Ionic Surfactants, *Langmuir*, 2015, **31**(3), 970–981.
- 27 M. Lee, U. H. Choi, R. H. Colby and H. W. Gibson, Ion Conduction in Imidazolium Acrylate Ionic Liquids and their Polymers, *Chem. Mater.*, 2010, **22**(21), 5814–5822.
- 28 U. H. Choi, Y. Ye, D. Salas de la Cruz, W. Liu, K. I. Winey, Y. A. Elabd, J. Runt and R. H. Colby, Dielectric and Viscoelastic Responses of Imidazolium-Based Ionomers with Different Counterions and Side Chain Lengths, *Macromolecules*, 2014, **47**(2), 777–790.
- 29 U. H. Choi, M. Lee, S. Wang, W. Liu, K. I. Winey, H. W. Gibson and R. H. Colby, Ionic Conduction and Dielectric Response of Poly(imidazolium acrylate) Ionomers, *Macromolecules*, 2012, **45**(9), 3974–3985.
- 30 Y. Ye and Y. A. Elabd, Anion exchanged polymerized ionic liquids: High free volume single ion conductors, *Polymer*, 2011, **52**(5), 1309–1317.
- 31 V. Bocharova, Z. Wojnarowska, P.-F. Cao, Y. Fu, R. Kumar, B. Li, V. N. Novikov, S. Zhao, A. Kisliuk, T. Saito, J. W. Mays, B. G. Sumpter and A. P. Sokolov, Influence of Chain Rigidity and Dielectric Constant on the Glass Transition Temperature in Polymerized Ionic Liquids, *J. Phys. Chem. B*, 2017, **121**(51), 11511–11519.
- 32 Y. Fu, V. Bocharova, M. Ma, A. P. Sokolov, B. G. Sumpter and R. Kumar, Effects of counterion size and backbone rigidity on the dynamics of ionic polymer melts and glasses, *Phys. Chem. Chem. Phys.*, 2017, **19**(40), 27442–27451.
- 33 Y. Cheng, J. Yang, J.-H. Hung, T. K. Patra and D. S. Simmons, Design Rules for Highly Conductive Polymeric Ionic Liquids from Molecular Dynamics Simulations, *Macromolecules*, 2018, **51**(17), 6630–6644.
- 34 B. Doughty, A.-C. Genix, I. Popov, B. Li, S. Zhao, T. Saito, D. A. Lutterman, R. L. Sacchi, B. G. Sumpter, Z. Wojnarowska and V. Bocharova, Structural correlations tailor conductive properties in polymerized ionic liquids, *Phys. Chem. Chem. Phys.*, 2019, **21**(27), 14775–14785.
- 35 J. R. Keith, N. J. Rebello, B. J. Cowen and V. Ganesan, Influence of Counterion Structure on Conductivity of Polymerized Ionic Liquids, *ACS Macro Lett.*, 2019, **8**(4), 387–392.
- 36 A. Hanisch, A. H. Gröschel, M. Förtsch, M. Drechsler, H. Jinnai, T. M. Ruhland, F. H. Schacher and A. H. E. Müller, Counterion-Mediated Hierarchical Self-Assembly of an ABC Miktoarm Star Terpolymer, *ACS Nano*, 2013, **7**(5), 4030–4041.
- 37 H. Cui, Z. Chen, K. L. Wooley and D. J. Pochan, Controlling Micellar Structure of Amphiphilic Charged Triblock Copolymers in Dilute Solution via Coassembly with Organic Counterions of Different Spacer Lengths, *Macromolecules*, 2006, **39**(19), 6599–6607.
- 38 Z. Zhang, M. M. Rahman, C. Abetz, B. Bajer, J. Wang and V. Abetz, Quaternization of a Polystyrene-block-poly(4-vinylpyridine) Isoporous Membrane: An Approach to Tune the Pore Size and the Charge Density, *Macromol. Rapid Commun.*, 2019, **40**(3), 1800729.
- 39 M. Billing, J. K. Elter and F. H. Schacher, Sulfo- and carboxybetaine-containing polyampholytes based on poly(2-vinylpyridine)s: Synthesis and solution behavior, *Polymer*, 2016, **104**, 40–48.
- 40 C. Facciotti, V. Saggiomo, A. Bunschoten, R. Fokkink, J. B. T. Hove, J. Wang and A. H. Velders, Cyclodextrin-based complex coacervate core micelles with tuneable supramolecular host–guest, metal-to-ligand and charge interactions, *Soft Matter*, 2018, **14**(47), 9542–9549.
- 41 H. M. van der Kooij, E. Spruijt, I. K. Voets, R. Fokkink, M. A. Cohen Stuart and J. van der Gucht, On the Stability and Morphology of Complex Coacervate Core Micelles:



- From Spherical to Wormlike Micelles, *Langmuir*, 2012, **28**(40), 14180–14191.
- 42 T. Pelras, A. Eisenga, G. Érsek, A. Altomare, G. Portale, M. Kamperman and K. Loos, One-Pot Synthesis of Strong Anionic/Charge-Neutral Amphiphilic Block Copolymers, *ACS Macro Lett.*, 2023, **12**(8), 1071–1078.
 - 43 A. H. Hofman, R. Fokkink and M. Kamperman, A mild and quantitative route towards well-defined strong anionic/hydrophobic diblock copolymers: synthesis and aqueous self-assembly, *Polym. Chem.*, 2019, **10**(45), 6109–6115.
 - 44 Y. S. Vygodskii, O. A. Mel'nik, A. S. Shaplov, E. I. Lozinskaya, I. A. Malyshkina and N. D. Gavrilova, Synthesis and ionic conductivity of polymer ionic liquids, *Polym. Sci., Ser. A*, 2007, **49**(3), 256–261.
 - 45 J. Yuan, D. Mecerreyes and M. Antonietti, Poly(ionic liquid)s: An update, *Prog. Polym. Sci.*, 2013, **38**(7), 1009–1036.
 - 46 J. Kolomanska, P. Johnston, A. Gregori, I. Fraga Domínguez, H.-J. Egelhaaf, S. Perrier, A. Rivaton, C. Dagron-Lartigau and P. D. Topham, Design, synthesis and thermal behaviour of a series of well-defined clickable and triggerable sulfonate polymers, *RSC Adv.*, 2015, **5**(82), 66554–66562.
 - 47 M. Aubin and R. E. Prud'homme, Analysis of the glass transition temperature of miscible polymer blends, *Macromolecules*, 1988, **21**(10), 2945–2949.
 - 48 M. Sedláč, Generation of multimacroion domains in polyelectrolyte solutions by change of ionic strength or pH (macroion charge), *J. Chem. Phys.*, 2002, **116**(12), 5256–5262.
 - 49 R. Hoogenboom, R. Becer, C. Guerrero-Sanchez, S. Hoepfner and U. S. Schubert, Solubility and Thermoresponsiveness of PMMA in Alcohol-Water Solvent Mixtures, *Aust. J. Chem.*, 2010, **63**(8), 1173–1178.
 - 50 R. Hoogenboom, S. Rogers, A. Can, R. Becer, C. Guerrero-Sanchez, D. Wouters, C. Hoepfner and U. S. Schubert, Self-assembly of double hydrophobic block copolymers in water-ethanol mixtures: from micelles to thermoresponsive micellar gels, *Chem. Commun.*, 2009, 5582–5584.

